Acta Crystallographica Section C
**Crystal Structure Communications**
ISSN 0108-2701

# Modulating the preferred O—H···O hydrogen-bonding motif in a conformationally constrained environment through hydroxy-group derivatization

**Goverdhan Mehta* and Saikat Sen**

Department of Organic Chemistry, Indian Institute of Science, Bangalore 560 012, Karnataka, India
Correspondence e-mail: gm@orgchem.iisc.ernet.in

Received 11 November 2009
Accepted 21 December 2009
Online 8 January 2010

The crystal structures of three conformationally locked esters, namely the centrosymmetric tetrabenzoate of all-axial perhydronaphthalene-2,3,4a,6,7,8a-hexaol, *viz. trans*-4a,8a-dihydroxyperhydronaphthalene-2,3,6,7-tetrayl tetrabenzoate, $C_{38}H_{34}O_{10}$, and the diacetate and dibenzoate of all-axial perhydronaphthalene-2,3,4a,8a-tetraol, *viz.* (2*R**,3*R**,4a*S**,8a*S**)-4a,8a-dihydroxyperhydronaphthalene-2,3-diyl diacetate, $C_{14}H_{22}O_6$, and (2*R**,3*R**,4a*S**,8a*S**)-4a,8a-dihydroxyperhydronaphthalene-2,3-diyl dibenzoate, $C_{24}H_{26}O_6$, have been analyzed in order to examine the preference of their supramolecular assemblies towards competing inter- and intramolecular O—H···O hydrogen bonds. It was anticipated that the supramolecular assembly of the esters under study would adopt two principal hydrogen-bonding modes, namely one that employs intermolecular O—H···O hydrogen bonds (mode 1) and another that sacrifices those for intramolecular O—H···O hydrogen bonds and settles for a crystal packing dictated by weak intermolecular interactions alone (mode 2). Thus, while the molecular assembly of the two crystalline diacyl derivatives conformed to a combination of hydrogen-bonding modes 1 and 2, the crystal packing in the tetrabenzoate preferred to follow mode 2 exclusively.

## Comment

We had envisaged in a recent communication that supramolecular assemblies of the all-axial tetraacyl derivatives (I) of the conformationally locked hexol (II) (Mehta, Sen & Ramesh, 2007; Mehta, Sen & Venkatesan, 2007), bearing chemodifferentiated secondary and tertiary OH groups, would evolve along two principal hydrogen-bonding modes (Mehta & Sen, 2009*a*). The first follows the hierarchy of the strength of the noncovalent interactions available in the ester (I) and opts for a crystal structure dictated mostly by intermolecular O—H···O hydrogen bonds, employing albeit the lesser accessible tertiary hydroxy groups (mode 1). The second scheme relegates the central OH groups to function merely as intramolecular O—H···O hydrogen-bond donors to the ester O atoms and settles in consequence for a crystal packing dictated by weak intermolecular interactions alone (mode 2). It would be logical to believe that the pattern of hydrogen bonding observed experimentally in the crystal structures of such esters as (I) would eventually depend on (*a*) the crystallization conditions employed and (*b*) the extent to which the peripheral ester groups can sequester the central hydroxy groups. For example, we have already demonstrated that the tetraacetate (III), which otherwise crystallizes along mode 1 when pure, can be goaded to follow mode 2 in a crystallization milieu, suitably doped with a molecular additive that inhibits mode 1 (Mehta & Sen, 2009*b*). In continuation, the present study compares the solid-state self-assemblies of the esters (IV)–(VI) with the intent of analyzing the scope of modulating the preferred hydrogen-bonding mode through variation in the steric environment around the central tertiary hydroxy groups. From a synthetic perspective, our choice of the OH-protecting functionalities, namely the acetyl and benzoyl groups in (IV)–(VI), was governed by the ease in their introduction (even in a sterically encumbered position) and purification, and the well documented crystallizability of the esters thus obtained.

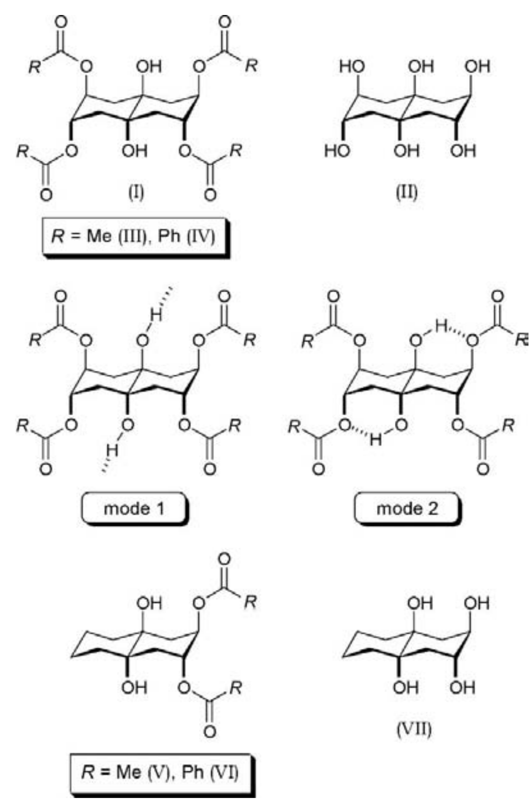


The diacetate (V) was prepared from the tetrol (VII) (Mehta, Sen & Ramesh, 2007) *via* base-mediated acetylation of the secondary hydroxy groups in an acetic anhydride–4-(dimethylamino)pyridine mixture. Benzoylation of the polyols (II) and (VII) was conveniently carried out in almost

 doi:10.1107/S0108270109054870  

quantitative yield in the presence of benzoyl chloride and pyridine.

The tetrabenzoate (IV) crystallized as small cuboidal blocks, with well defined faces, at ambient temperature from its solution in a 2:1:1 chloroform–benzene–petroleum ether mixture. Its crystal structure was solved and refined in the centrosymmetric monoclinic space group $P2_1/c$ ($Z = 2$), with the $C_{2h}$ symmetric tetrabenzoate molecules occupying the crystallographic inversion centers at ($\frac{1}{2}$, $\frac{1}{2}$, 0) and ($\frac{1}{2}$, 0, $\frac{1}{2}$) (Fig. 1). Following mode 2, the hydroxy groups in (IV) engage in intramolecular O—H···O hydrogen bonding, while intermolecular C—H···O hydrogen bonds link the tetrabenzoate molecules to form chains parallel to the *c* axis (Fig. 2 and Table 1).

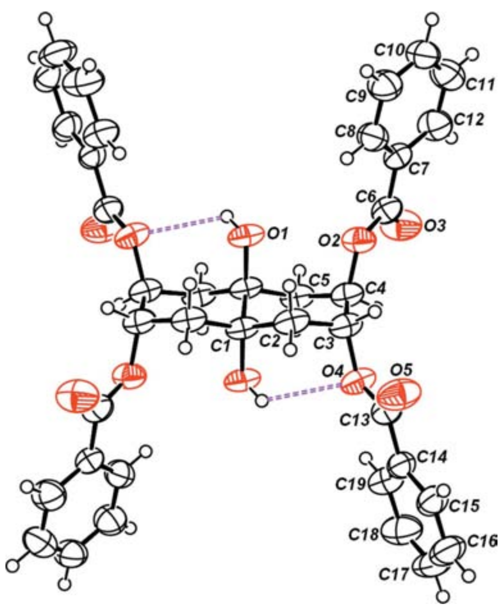


**Figure 1**
A view of the tetrabenzoate (IV), showing the atom-numbering scheme. Displacement ellipsoids for non-H atoms are drawn at the 50% probability level. H atoms are shown as small spheres of arbitrary radii. The dashed lines indicate intramolecular O—H···O hydrogen bonds.

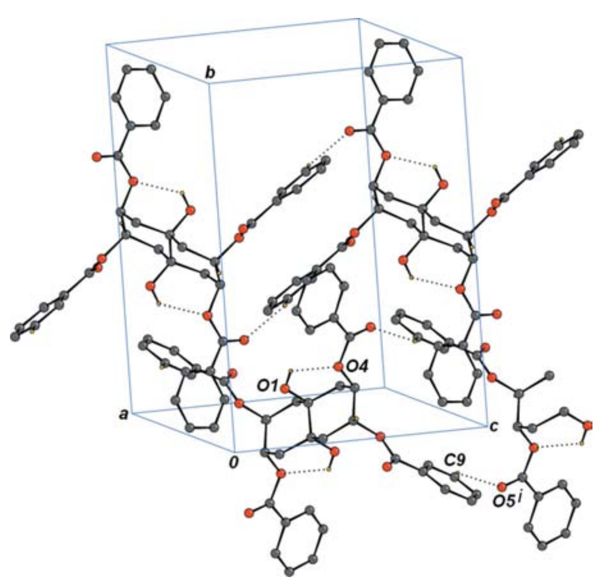


**Figure 2**
The molecular packing of (IV). H atoms not involved in hydrogen bonding have been omitted for clarity. Dotted lines indicate hydrogen bonds. [Symmetry code: (i) $-x + 1$, $-y$, $-z + 2$.]

Crystals of the diacetate (V) suitable for single-crystal X-ray diffraction analysis were obtained as extremely thin needles by allowing a hot solution of (V) in a 1:20 ethyl acetate–petroleum ether mixture to slowly attain ambient temperature. Packing in the centrosymmetric monoclinic space group $P2_1/n$ ($Z = 4$), the $C_2$ symmetric molecules of the diacetate (V) adopt a supramolecular assembly that essentially follows a combination of both modes 1 and 2 (Fig. 3). Thus, one of the two tertiary hydroxy groups in (V) functions as both an intramolecular hydrogen-bond donor and an acceptor for intermolecular O—H···O hydrogen bonds that link the diacetate molecules into chains essentially along the [101] direction (Fig. 4 and Table 2). The molecular chains thus formed are held together by weak van der Waals interactions.

Obtaining crystals of the dibenzoate (VI) suitable for single-crystal X-ray diffraction analysis presented a particular challenge on account of its tendency to form flocculent microcrystalline masses in solution and its high solubility, even in solvents of low polarity such as petroleum ether. After several trials, the dibenzoate (VI) was obtained eventually as tiny scales by nucleating a saturated solution of (VI) in benzene, with the microcrystals obtained by slow evaporation of its dilute solution in petroleum ether. X-ray diffraction data collected on (VI) at 291 K revealed that the $C_2$ symmetric dibenzoate crystallized in the centrosymmetric monoclinic space group $P2_1/c$ ($Z = 4$), following an O—H···O hydrogen-bonding pattern akin to that observed for the diacetate (V)

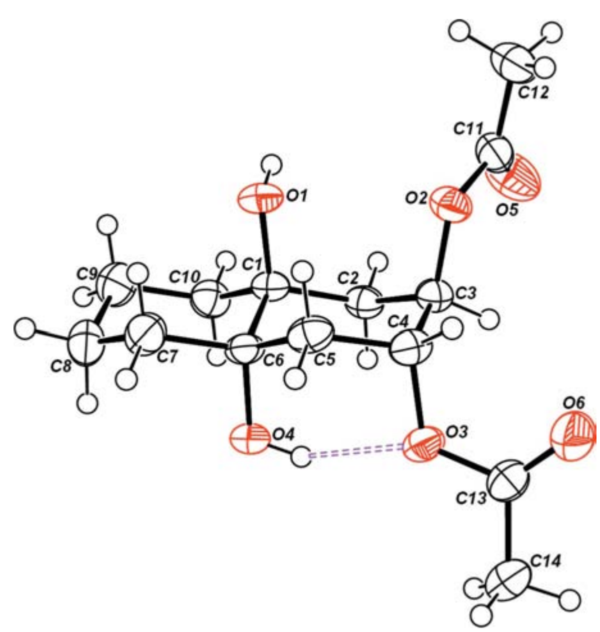


**Figure 3**
A view of the diacetate (V), showing the atom-numbering scheme. Displacement ellipsoids for non-H atoms are drawn at the 50% probability level. H atoms are shown as small spheres of arbitrary radii. The dashed line indicates the intramolecular O—H···O hydrogen bond.

(Fig. 5). Thus, intermolecular O—H···O hydrogen bonds among the tertiary hydroxy groups, one of which participates additionally in intramolecular hydrogen bonding, link the dibenzoate molecules into columnar architectures running parallel to the *c* axis (Fig. 6 and Table 3). These are in turn held in the crystal structure by weak van der Waals interactions.

We have therefore analyzed the solid-state self-assemblies of the tetrabenzoate (IV), derived from the conformationally locked hexol (II), and the diacyl derivatives, *viz*. the diacetate (V) and the dibenzoate (VI), of the annulated polycyclitol (VII) (Mehta & Ramesh, 2000, 2001). As already alluded to, the present study was directed towards discerning a possible connection between the extent of steric shielding of the central OH groups by the flanking ester groups, and the preference of supramolecular assemblies of crystalline esters of (II) for competing inter- and intramolecular O—H···O hydrogen bonds (Bilton *et al.*, 2000; Baudron *et al.*, 2004; Borho *et al.*, 2006). Thus, while a pure sample of the tetraacetate (III) prefers to engage the tertiary OH groups as intermolecular O—H···O hydrogen bonding (mode 1), that of the tetrabenzoate (IV) conforms exclusively to mode 2 and relegates the hydroxy functionalities to serve as intramolecular O—H···O hydrogen-bond donors. The difference observed in the favored hydrogen-bonding mode in (III) and (IV) would appear to stem not only from the larger bulk of the phenyl group in (IV), as compared with the methyl group in (III), but also from the ability of the aromatic group in (IV) to engage in stronger C—H···O hydrogen bonds (Desiraju & Steiner, 1999). The individualistic nature of the self-assemblies of (III) and (IV) should be compared with the stark commonalities observed in the molecular packing of the diacyl derivatives (V) and (VI). Relieved of the constraints of the site symmetry and steric bulk of two acyl groups, the esters (V) and (VI) exhibit crystal structures that follow a combination of modes 1 and 2. It is also interesting to note that this hydrogen-bonding preference and formation of the columnar architectures in the self-assemblies of (V) and (VI) not only optimizes the stronger O—H···O hydrogen bonds within each column, but also maximizes the weaker van der Waals interactions among the hydrophobic groups of adjacent columns (Alfonso *et al.*, 2009; Mehta & Sen, 2005; 2008).

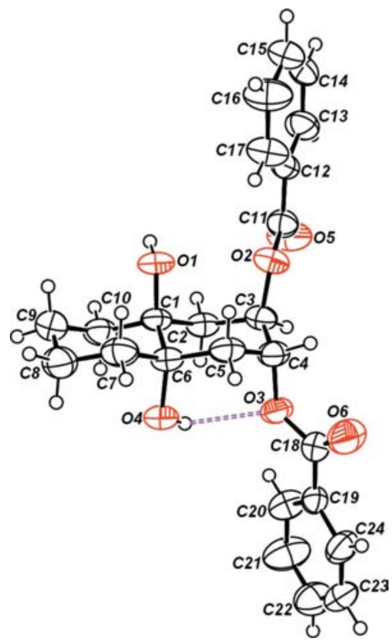


**Figure 5**
A view of the dibenzoate (VI), showing the atom-numbering scheme. Displacement ellipsoids for non-H atoms are drawn at the 50% probability level. H atoms are shown as small spheres of arbitrary radii. The dashed line indicates the intramolecular O—H···O hydrogen bond.

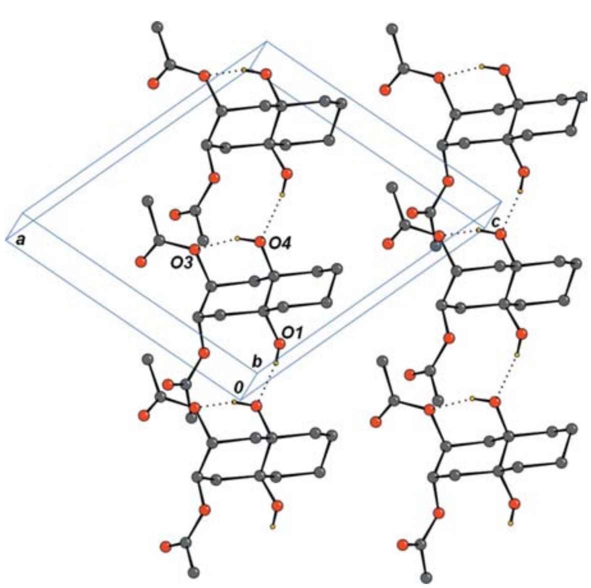


**Figure 4**
The molecular packing of (V). H atoms bonded to C atoms have been omitted for clarity. Dotted lines indicate hydrogen bonds.

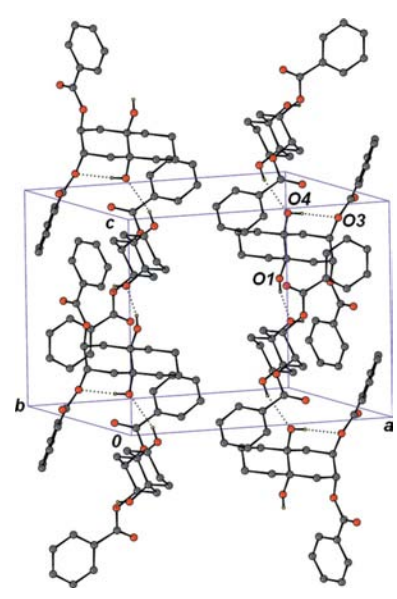


**Figure 6**
The molecular packing of (VI). H atoms bonded to C atoms have been omitted for clarity. Dotted lines indicate hydrogen bonds.

In summary, the conformationally locked *trans*-decalin framework, bearing spatially fixed and chemodifferentiated functionalities, has been employed as a probe for studying the effect that structural or functional variations in the substituents can have on the self-assembly process. In this vein, the present study highlights that O—H···O hydrogen-bonding preferences, and thus the mode of molecular packing in axial-rich polycyclitols, can be fine-tuned through suitable derivatization of the hydroxy groups.

## Experimental

Freshly distilled benzoyl chloride (121 mg, 100 µl, 0.861 mmol) was added to a suspension of a finely ground sample (46 mg, 0.196 mmol) of the hexol (II) in dry dichloromethane (3 ml). The reaction mixture was stirred at ambient temperature for 2 h, after which time pyridine (155 mg, 160 µl, 1.966 mmol) was added dropwise and the reaction was allowed to proceed at ambient temperature for 8 h. During this interval, the heavy suspension of the hexol (II) in dichloromethane is gradually replaced by a lighter precipitate of pyridinium chloride, and the odor of benzoyl chloride becomes almost imperceptible. The reaction was quenched with saturated sodium bicarbonate solution and the product extracted with dichloromethane. The combined organic extracts were washed with dilute HCl solution and brine, and finally dried over anhydrous sodium sulfate. Evaporation of the solvent afforded the crude product, which was purified by column chromatography over silica gel using 30% ethyl acetate–petroleum ether to obtain the tetrabenzoate (IV) (125 mg, 98%) as a colorless solid [m.p. 550.6–551.4 K (uncorrected)].

A solution of the tetrol (VII) (25 mg, 0.124 mmol) and 4-(dimethylamino)pyridine (36 mg, 0.297 mmol) in acetic anhydride (0.5 ml) was stirred at ambient temperature for 3 h. The reaction was then cooled to 273 K and quenched with methanol (0.5 ml). The volatiles were removed under vacuum and the crude product obtained purified by column chromatography over silica gel using 60% ethyl acetate–petroleum ether to obtain the diacetate (V) [30 mg, 86%; m.p. 398.1–398.4 K (uncorrected)].

Freshly distilled benzoyl chloride (36 mg, 30 µl, 0.260 mmol), followed by pyridine (24 mg, 25 µl, 0.309 mmol), was added to a solution of the tetrol (VII) (25 mg, 0.124 mmol) in dichloromethane (2 ml) and the reaction mixture thus obtained was stirred at ambient temperature for 4 h. The reaction was then quenched with saturated sodium bicarbonate solution (1 ml) and the product extracted with dichloromethane. The combined organic extracts were washed with dilute HCl solution and brine, and finally dried over anhydrous sodium sulfate. Evaporation of the solvent and subsequent purification by column chromatography over silica gel using 20% ethyl acetate–petroleum ether gave the dibenzoate (VI) (50 mg, 99%) as a fluffy solid [m.p. 447.3–447.7 K (uncorrected)]. The conditions for growing diffraction quality crystals of (IV)–(VI) are presented in the *Comment* section.

### Compound (IV)

*Crystal data*

| | |
|---|---|
| $C_{38}H_{34}O_{10}$ | $V$ = 1607.6 (9) Å$^3$ |
| $M_r$ = 650.65 | $Z$ = 2 |
| Monoclinic, $P2_1/c$ | Mo $K\alpha$ radiation |
| $a$ = 9.734 (3) Å | $\mu$ = 0.10 mm$^{-1}$ |
| $b$ = 15.993 (5) Å | $T$ = 291 K |
| $c$ = 10.827 (4) Å | 0.22 × 0.18 × 0.15 mm |
| $\beta$ = 107.488 (5)° | |

*Data collection*

| | |
|---|---|
| Bruker SMART APEX CCD area-detector diffractometer | 11704 measured reflections |
| Absorption correction: multi-scan (*SADABS*; Sheldrick, 2003) | 2934 independent reflections |
| $T_{min}$ = 0.936, $T_{max}$ = 0.974 | 2036 reflections with $I > 2\sigma(I)$ |
| | $R_{int}$ = 0.028 |

*Refinement*

| | |
|---|---|
| $R[F^2 > 2\sigma(F^2)]$ = 0.045 | 218 parameters |
| $wR(F^2)$ = 0.118 | H-atom parameters constrained |
| $S$ = 1.03 | $\Delta\rho_{max}$ = 0.14 e Å$^{-3}$ |
| 2934 reflections | $\Delta\rho_{min}$ = −0.18 e Å$^{-3}$ |

**Table 1**
Hydrogen-bond geometry (Å, °) for (IV).

| $D$—H···$A$ | $D$—H | H···$A$ | $D$···$A$ | $D$—H···$A$ |
|---|---|---|---|---|
| O1—H1$O$···O4 | 0.82 | 2.44 | 2.921 (2) | 118 |
| C9—H9···O5$^{i}$ | 0.93 | 2.50 | 3.201 (3) | 132 |

Symmetry code: (i) $-x+1, -y, -z+2$.

### Compound (V)

*Crystal data*

| | |
|---|---|
| $C_{14}H_{22}O_6$ | $V$ = 1423.2 (17) Å$^3$ |
| $M_r$ = 286.32 | $Z$ = 4 |
| Monoclinic, $P2_1/n$ | Mo $K\alpha$ radiation |
| $a$ = 9.888 (7) Å | $\mu$ = 0.10 mm$^{-1}$ |
| $b$ = 14.747 (10) Å | $T$ = 291 K |
| $c$ = 10.417 (7) Å | 0.32 × 0.09 × 0.04 mm |
| $\beta$ = 110.444 (10)° | |

*Data collection*

| | |
|---|---|
| Bruker SMART APEX CCD area-detector diffractometer | 10468 measured reflections |
| Absorption correction: multi-scan (*SADABS*; Sheldrick, 2003) | 2636 independent reflections |
| $T_{min}$ = 0.955, $T_{max}$ = 0.996 | 2125 reflections with $I > 2\sigma(I)$ |
| | $R_{int}$ = 0.026 |

*Refinement*

| | |
|---|---|
| $R[F^2 > 2\sigma(F^2)]$ = 0.042 | 185 parameters |
| $wR(F^2)$ = 0.104 | H-atom parameters constrained |
| $S$ = 1.03 | $\Delta\rho_{max}$ = 0.21 e Å$^{-3}$ |
| 2636 reflections | $\Delta\rho_{min}$ = −0.16 e Å$^{-3}$ |

**Table 2**
Hydrogen-bond geometry (Å, °) for (V).

| $D$—H···$A$ | $D$—H | H···$A$ | $D$···$A$ | $D$—H···$A$ |
|---|---|---|---|---|
| O1—H1$O$···O4$^{i}$ | 0.82 | 2.07 | 2.882 (2) | 168 |
| O4—H4$O$···O3 | 0.82 | 2.06 | 2.769 (2) | 145 |

Symmetry code: (i) $x-\frac{1}{2}, -y+\frac{1}{2}, z-\frac{1}{2}$.

### Compound (VI)

*Crystal data*

| | |
|---|---|
| $C_{24}H_{26}O_6$ | $V$ = 2144.4 (7) Å$^3$ |
| $M_r$ = 410.45 | $Z$ = 4 |
| Monoclinic, $P2_1/c$ | Mo $K\alpha$ radiation |
| $a$ = 16.246 (3) Å | $\mu$ = 0.09 mm$^{-1}$ |
| $b$ = 11.167 (2) Å | $T$ = 291 K |
| $c$ = 11.829 (2) Å | 0.17 × 0.14 × 0.02 mm |
| $\beta$ = 92.219 (6)° | |

*Data collection*

Bruker SMART APEX CCD area-detector diffractometer
Absorption correction: multi-scan (*SADABS*; Sheldrick, 2003)
$T_{min} = 0.948$, $T_{max} = 0.998$
16433 measured reflections
3594 independent reflections
1295 reflections with $I > 2\sigma(I)$
$R_{int} = 0.135$

*Refinement*

$R[F^2 > 2\sigma(F^2)] = 0.047$
$wR(F^2) = 0.112$
$S = 0.92$
3594 reflections
271 parameters
H-atom parameters constrained
$\Delta\rho_{max} = 0.13$ e Å$^{-3}$
$\Delta\rho_{min} = -0.14$ e Å$^{-3}$

**Table 3**
Hydrogen-bond geometry (Å, °) for (VI).

| $D$—H⋯$A$ | $D$—H | H⋯$A$ | $D$⋯$A$ | $D$—H⋯$A$ |
|---|---|---|---|---|
| O1—H1$O$⋯O4$^{i}$ | 0.82 | 2.22 | 3.013 (3) | 163 |
| O4—H4$O$⋯O3 | 0.82 | 2.22 | 2.825 (2) | 131 |

Symmetry code: (i) $x, -y+\frac{1}{2}, z-\frac{1}{2}$.

The aromatic, methine (CH) and methylene ($CH_2$) H atoms were placed in geometrically idealized positions and allowed to ride on their parent atoms, with C—H distances in the range 0.93–0.98 Å and $U_{iso}$(H) values of $1.2U_{eq}$(C). The $CH_3$ and OH H atoms were constrained to an ideal geometry, with C—H distances of 0.96 Å, O—H distances fixed at 0.82 Å and $U_{iso}$(H) values of $1.5U_{eq}$(C,O). During refinement, however, each methyl and hydroxy group was allowed to rotate freely about the respective C—C or C—O bond.

For all compounds, data collection: *SMART* (Bruker, 1998); cell refinement: *SAINT* (Bruker, 1998); data reduction: *SAINT*; program(s) used to solve structure: *SIR92* (Altomare *et al.*, 1994); program(s) used to refine structure: *SHELXL97* (Sheldrick, 2008); molecular graphics: *ORTEP-3 for Windows* (Farrugia, 1997) and *CAMERON* (Watkin *et al.*, 1993); software used to prepare material for publication: *PLATON* (Spek, 2009).

We thank DST, India, for the CCD facility at IISc, Bangalore. GM thanks CSIR, India, for research support and the award of the Bhatnagar Fellowship.

Supplementary data for this paper are available from the IUCr electronic archives (Reference: TR3062). Services for accessing these data are described at the back of the journal.

## References

Alfonso, I., Bolte, M., Bru, M., Burguete, M. I. & Luis, S. V. (2009). *CrystEngComm*, **11**, 735–738.
Altomare, A., Cascarano, G., Giacovazzo, C., Guagliardi, A., Burla, M. C., Polidori, G. & Camalli, M. (1994). *J. Appl. Cryst.* **27**, 435.
Baudron, S. A., Avarvari, N., Canadell, E., Auban-Senzier, P. & Batail, P. (2004). *Chem. Eur. J.* **10**, 4498–4511.
Bilton, C., Allen, F. H., Shields, G. P. & Howard, J. A. K. (2000). *Acta Cryst.* B**56**, 849–856.
Borho, N., Suhm, M. A., Le Barbu-Debus, K. & Zehnacker, A. (2006). *Phys. Chem. Chem. Phys.* **8**, 4449–4460.
Bruker (1998). *SMART* (Version 6.028) and *SAINT* (Version 6.02). Bruker AXS Inc., Madison, Wisconsin, USA.
Desiraju, G. R. & Steiner, T. (1999). *The Weak Hydrogen Bond in Structural Chemistry and Biology.* Oxford University Press.
Farrugia, L. J. (1997). *J. Appl. Cryst.* **30**, 565.
Mehta, G. & Ramesh, S. S. (2000). *Chem. Commun.* pp. 2429–2430.
Mehta, G. & Ramesh, S. S. (2001). *Tetrahedron Lett.* **42**, 1987–1990.
Mehta, G. & Sen, S. (2005). *CrystEngComm*, **7**, 656–663.
Mehta, G. & Sen, S. (2009*a*). *Chem. Commun.* pp. 5981–5983.
Mehta, G. & Sen, S. (2009*b*). *Tetrahedron*, **65**, 9713–9718.
Mehta, G., Sen, S. & Pallavi, K. (2008). *CrystEngComm*, **10**, 534–540.
Mehta, G., Sen, S. & Ramesh, S. S. (2007). *Eur. J. Org. Chem.* pp. 423–436.
Mehta, G., Sen, S. & Venkatesan, K. (2007). *CrystEngComm*, **9**, 144–151.
Sheldrick, G. M. (2003). *SADABS*. Version 2.10. University of Göttingen, Germany.
Sheldrick, G. M. (2008). *Acta Cryst.* A**64**, 112–122.
Spek, A. L. (2009). *Acta Cryst.* D**65**, 148–155.
Watkin, D. M., Pearce, L. & Prout, C. K. (1993). *CAMERON*. Chemical Crystallography Laboratory, University of Oxford, England.